02,07,13

# Ultimate parameters of SIS junctions in theory and technological possibilities to achieve them

© M.A. Tarasov[1], A.A. Lomov[2], A.M. Chekushkin[1], A.A. Gunbina[3], M.Yu. Fominsky[1], S.V. Kraevsky[4], R.K. Kozulin[1], A.V. Shadrin[5]

[1] Kotelnikov Institute of Radio Engineering and Electronics, Russian Academy of Sciences, Moscow, Russia
[2] Valiev Institute of Physics and Technology, Russian Academy of Sciences, Moscow, Russia
[3] Institute of Applied Physics, Russian Academy of Sciences, Nizhny Novgorod, Russia
[4] Institute of Biomedical Chenistry named after V.N. Orekhovich, Moscow, Russia
[5] Moscow Institute of Physics and Technology, Dolgoprudny, Moscow region, Russia

E-mail: tarasov@hitech.cplire.ru

*Received April 17, 2023*
*Revised April 17, 2023*
*Accepted May 11, 2023*

Tunneling Josephson junctions of the superconductor-insulator-superconductor (SIS) type have a history of more than 50 years, and theoretical estimates of the ultimate parameters of devices for receiving and processing signals based on them look very promising. In practice, in many cases, the actually achieved parameters turn out to be much worse than the theoretical ones, so for niobium SQUIDs the characteristic voltage $V_c = I_c R_n$ at best reaches $200\,\mu$V, and according to theory it should be up to 2 mV. For Terahertz SIS mixers and oscillators, the main problems are a large specific capacitance, hysteresis, and leakage currents. These problems may be related to the morphology and crystal structure of superconductor films. In practice, films are granular, tunnel barriers are nonuniform, the effective area is about 10% of geometric area, leakage currents, parasitic capacitances occur. The crystal structure determines fundamentally different properties of the same elements, for example, for carbon it is diamond, graphite, fullerenes, nanotubes. Important components of a promising superconducting technology are: the use of single-crystal substrates matched in lattice constant and orientation with the grown films, optimization of growth temperature conditions, controlled formation of an oxide or nitride tunnel barrier. One option is to use a Schottky barrier for the semiconductor interlayer instead of a dielectric or normal metal one. This review presents the results of studying films by X-ray diffraction diagnostics, atomic force microscopy, and electron microscopy, showing the main bottlenecks of the existing technology with the deposition of niobium, niobium nitride, and aluminum films on oxidized standard silicon substrates, as well as the results of quasi-epitaxial growth of films on single-crystal substrates at various temperature conditions. Reproducible manufacturing of high-quality tunnel junctions can be achieved by implementing atomically smooth surfaces of tunnel contacts, which will improve the signal and noise characteristics of superconducting devices for receiving and processing information.

**Keywords:** Josephson junctions, tunnel junctions, crystal structure, epitaxial films, surface roughness, single crystal substrates.

DOI: 10.21883/PSS.2023.07.56396.29H

## 1. Expected parameters of structures

Parameters of tunnel SIS junctions to a large extent are defined by the structure of the barrier area from aluminium oxide or nitride. For practical tunnel junctions with asymptotic resistance $R_n S = (1 \ldots 2)\,\mathrm{k\Omega} \cdot \mu\mathrm{m}^2$, measured by LC-resonances, the specific capacity is from 70 to 50 $\mathrm{fF}/\mu\mathrm{m}^2$. According to formula for a flat capacitor $C = \varepsilon\varepsilon_0 S/d$, where $\varepsilon_0 = 8.85 \cdot 10^{-12}$ F/m and $\varepsilon = 3$, this corresponds to thickness of oxide barrier $d = \varepsilon\varepsilon_0 S/C = 0.38{-}0.5$ nm. For tunnel junction at such asymptotic resistances the estimated thickness of the barrier is approximately 1.8 nm, for the ideal flat capacitor that would correspond to the specific capacity 15 $\mathrm{fF}/\mu\mathrm{m}^2$, i. e. the difference in the estimate of thickness in theory is 4.7−3.6 times, i. e. the capacity is formed on a larger area compared to the effective area of the tunnel barrier. In reality the relative dielectric permittivity of even the ideal amorphous barrier is less than three, the effective thickness of the capacitance barrier will be at the level of 0.25 nm. One may suggest that the rough surface has much larger area with lower transparency. According to literature data [1] the effective tunneling area is downright 0.13. This means that only the smaller (thinner) part of the geometric area of the junction is responsible for the tunnel conductivity, and the remaining (the thicker part) defines the effective stray capacity. However, it is quite complicated to

**Table 1.** Theoretical estimates of parameters of tunnel junctions based on NbN/I/NbN and Al/I/Al with barrier thickness 1 nm, 2 nm and $\varepsilon = 3$

| Structure, oxide thickness | $J_c$ ($\mu$A/$\mu$m$^2$) | $R_n$ ($\Omega/\mu$m$^2$) | $V_c$ ($\mu$V) | $C$ (fF/$\mu$m$^2$) | $\beta_c$ | $\tau = RC$ (ps) | $f_{RC} = 1/2\pi\tau$ (THz) |
|---|---|---|---|---|---|---|---|
| NbN/I/NbN, oxide 1 nm | 250 | 5.6 | 1400 | 24 | 0.2 | 0.13 | 1 |
| NbN/I/NbN, oxide 2 nm | 0.022 | 63000 | 1380 | 13 | 1200 | 813 | 0.012 |
| Al/I/Al, oxide 1nm | 36 | 5.6 | 196 | 24 | 0.014 | 0.13 | 1 |
| Al/I/Al, oxide 2 nm | 0.003 | 6300 | 19 | 13 | 166 | 813 | 0.012 |

rely on the ideal tunnel barrier, since for single-crystal $Al_2O_3$ the real lattice constant measured by X-ray diffraction $a-b$ is 0.47 nm and along axis $c$, according to our estimates, makes 1.3 nm [2], i. e. the ideal junction will represent a tunnel barrier with thickness of approximately equal to the dielectric lattice constant. For this purpose it is necessary to form atomically smooth crystalline surface without defects and crystal twins. At the same time the area of junctions will be by order less than the standard junctions on granulated films at the same values of the tunnel transparency.

Transparency of the tunnel barrier [3] may be described by the ratio of output and input amplitudes of wave functions

$$\frac{F}{A} = 4\sqrt{\frac{U}{E}}\,\exp\left(-\frac{\sqrt{2mU}}{h}\,w\right),$$

where $U$ — barrier height, $E$ — electron energy, $m$ — electron mass, $w$ — barrier width. Conductivity is proportionate to the square of these amplitudes. For barrier height 1 eV, width 1 nm we get $(F/A)^2 = 4\cdot 10^{-4}$ and for 2 nm $(F/A)^2 = 10^{-8}$. This means that ratio of resistances $R_{2\,\mathrm{nm}}/R_{1\,\mathrm{nm}}$ will be $4\cdot 10^4$. For different dielectrics these rations will somewhat differ, because the barrier height may vary within the limits of several volts.

Density of critical current in NbN/AlN/NbN junction may be described by a simple empirical formula $J_c = A\exp(-10d_{\mathrm{AlN}}(\mathrm{nm}))$, which corresponds to barrier thickness 1.1 nm for 250 $\mu$A/$\mu$m$^2$ and 2 nm for 22 nA/$\mu$m$^2$. Critical current density for these two cases differs almost by 4 orders, and capacity differs by less than twice.

Capacitance hysteresis (do not confuse it with the thermal one!) may be described by McCumber parameter $\beta_c = I_cR^2C\cdot 4\pi e/h = (V_\Delta^2 C)/(I_c\Phi_o)$, at $\beta_c > 1$ current-voltage curve shows hysteresis. Calculating for niobium $I_cR = 0.5V_\Delta = 1.4$ mV we get $R_{250} = 5.6\,\Omega\cdot\mu$m$^2$ for 250 $\mu$A and $R_{0.022} = 63\,\mathrm{k}\Omega\cdot\mu\mathrm{m}^2$ for 22 nA. Corresponding capacities $C_{250} = 24$ fF and $C_{0.022} = 13$ fF. As a result the estimated McCumber parameter $\beta_{250} = 0.2$ and $\beta_{0.022} = 1200$. This is clear, the time constant $\tau = RC$ will make $\tau_{250} = 0.13$ ps and $\tau_{0.022} = 813$ ps, i. e. differs, as the critical current, by 4 orders. Low value of McCumber parameter of less than a unit means hysteresis-free current-voltage curve and does not require resistive shunting, i. e. makes it possible to fully implement the theoretical estimates for niobium junctions. For niobium nitride the difference from niobium is approximately 1.5 times.

For aluminium junctions it is necessary to replace the energy band gap value must be replaced for value $I_cR = 0.5V_\Delta = 0.2$ mV. At the same parameters of the tunnel barrier for resistance 5.6 $\Omega$ the critical current density per square micron will make 36 $\mu$A, and for 63 k$\Omega$ it will make 3 nA. The resulting McCumber parameter will be $\beta_{36} = 0.014$ and $\beta_{0.003} = 166$.

In the summary Table 1 there are theoretical estimates for tunnel junctions with area of 1 $\mu$m$^2$ and dielectric thickness 1 and 2 nm in SIS junctions based on niobium nitride and aluminium films.

Therefore, in case of successful solution to a problem of developing epitaxial atomically smooth superconducting tunnel junctions, it is possible to get rid of hysteresis and the need for resistive shunting of junctions, which means substantial improvement of all limit characteristics for devices of superconducting analog and digital electronics.

Methods of X-ray diffraction, electronic and atomic force microscopy provide information on element composition, crystalline structure and roughness of film surface. They make it possible to define microscopic defects, capable of considerable deterioration of signal and noise characteristics of superconducting quantum devices.

## 2. Films and tunnel structures based on niobium nitride

Our studies of SIS junctions Nb−AlN−NbN show that resulting films are quite rough, see Fig. 1. Grain size exceeds 100 nm.

The graphic picture of the niobium nitride film surface is given by image in an atomic force microscope (AFM), Fig. 2 shows grained rough structure.

Superconducting properties and crystalline structure of epitaxial single-crystal films of niobium nitride produced by HF magnetron sputtering at room temperature on (100) MgO substrate [4] are measured in NbN/AlN/Nb tunnel junctions. Electronic and X-ray diffraction demonstrated good crystalline properties and constant of lattice 0.445 nm. Close coupling parameter made $\alpha = 2\Delta_{\mathrm{NbN}}(0)/kT_c = 4.16$, where $k$ — Boltzmann constant, $T_c$ — critical temperature. London penetration depth of magnetic field $\lambda = 176$ nm.

Epitaxial films of NbN/AlN/NbN [5] were grown by reactive magnetron sputtering at DC at temperature of 830 and 450°C on planes $A$ and $C$ of sapphire and planes (001),

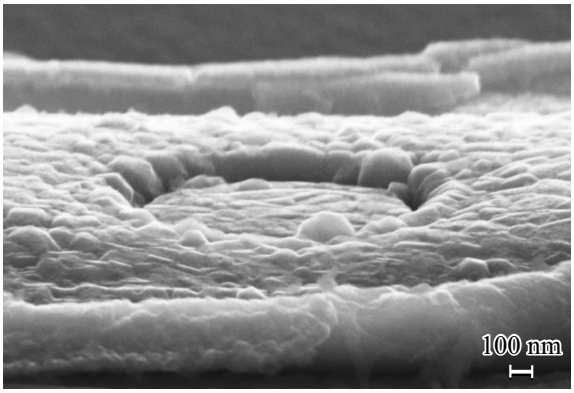


**Figure 1.** Image of Nb−AlN−NbN-junction with upper NbN.

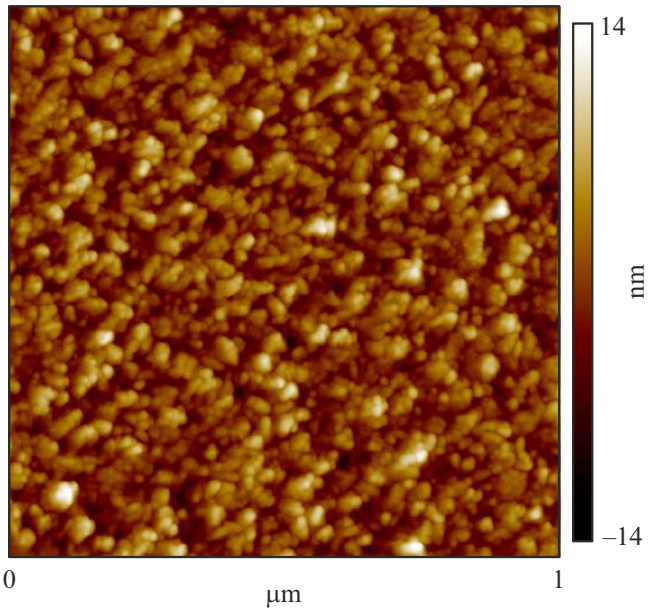


**Figure 2.** AFM-image of niobium nitride film surface.

(110), (111) MgO. Growths in the form of columns result in high roughness of the surface and prevent even growth of subsequent layers. In case of polycrystalline quartz substrate the NbN films become polycrystalline and non-textured, and AlN films are mostly amorphous. Surface roughness and grain size increase with film thickness growth. Single-crystal NbN films have cubic structure of lattice constant $a = 0.439$ nm, and AlN are usually hexagonal with $a = 0.311$ nm and $c = 0.498$ nm. Methods of transmission electron microscopy (TEM), electron energy loss spectroscopy (EELS) studied options for epitaxial growth of multilayer structures. It turned out that separately one may produce single-crystal films, but it is not always possible to grow a single-crystal multilayer structure. Substrates that make it possible to grow the first NbN layer in orientation (111) turn out to be preferable, since AlN grows (0001) on them, which provides for potential subsequent growth of NbN (111). It may turn out that sputtering of fine-crystalline films on polycrystalline quartz substrates will be smoother because of averaging in a multilayer structure, and the first NbN layer shall be made as thin as possible, since its roughness grows as the thickness grows.

Method of magnetron sputtering of NbN at DC with a nitrogen ion beam (ion beam assisted sputtering, IBAS) at room temperature onto silicon substrates was studied in [6]. Grain size was approximately 25 nm according to XRD and AFM measurements.

The objective of creating epitaxial NbN/AlN/NbN tunnel junctions of high quality was most closely approached in [7]. A three-layer structure was grown on MgO (100) substrates at temperature of not more than 100°C. A specific feature of the process was very low speed of AlN barrier application 0.05 nm/s. Critical current density was $250\,\mu\text{A}/\mu\text{m}^2$, $I_cR_n = 3.5$ mV. Cross section in the scanning transmission electron microscope (STEM) in such junctions demonstrates almost perfect epitaxial growth on the surface (100). AlN barrier with thickness of less than 2 nm grows epitaxially in a cubic phase above NbN, despite their difference in volume crystalline structures.

## 3. Niobium films and tunnel structures on its basis

Tunnel junctionsNb−AlO$x$−Nb are the main elements of the majority of modern superconductive electronic devices. Three-layer structure was made in a single vacuum cycle. Thickness of the bottom niobium layer was 200 nm, then the deposition of 7 nm of aluminum was performed, which later was oxidized at pressure of 1 mbar within 20 min, and after that the top niobium layer with thickness of 80 nm was deposited. SIS junction of the required area is formed using resistive mask, over which the reactive ion etching in $CF_4$ is performed in the top layer (Nb). Then the anodization of SIS junction faces in electrolyte solution is performed to prevent from micro short circuits. During the following vacuum cycle of deposition the contact layer (top electrode) made of aluminum with thickness of 350 nm, is formed over the new resistive mask.

Investigation of niobium films in an atomic force microscope shows high grain of regular films (see Fig. 3), besides, grains are of extended shape, in contrast to the round one for niobium nitride (Fig. 2).

There are multiple publications on the technology for application of thin niobium films and tunnel SIS junctions on their basis. Usually the critical current density does not exceed $10\,\mu\text{A}/\mu\text{m}^2$. Most developed classic technology was previously developed in HYPRES Inc. [8]. Nb/AlO$_x$/Nb tunnel junctions with critical current density $200\,\mu\text{A}/\mu\text{m}^2$ make it possible to implement logical keys with switching frequency of up to 400 GHz. A later paper [9] reports achievement of critical current density $600\,\mu\text{A}/\mu\text{m}^2$ in junctions with aluminium oxide with thickness of less than 1.1 nm. This makes it possible to get rid of resistive

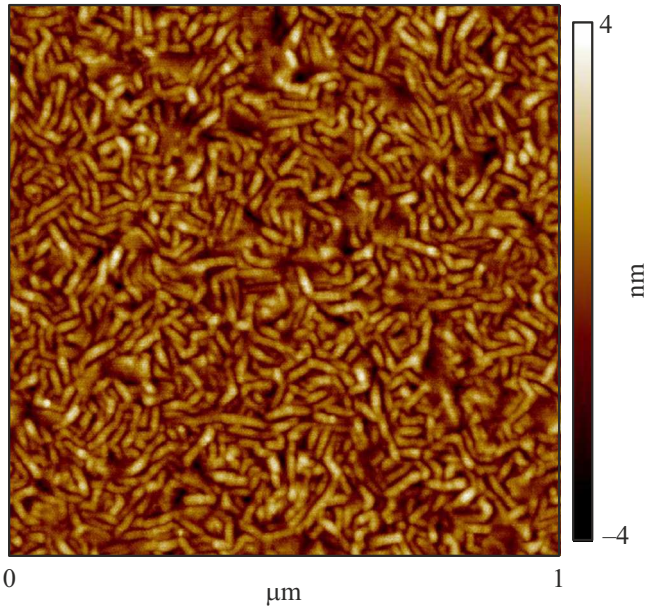


**Figure 3.** AFM-image of niobium film.

shunting of SIS junctions and to increase the specific junction frequency $f_c = V_c/\Phi_0$. Higher current density values up to 1.4 mA/$\mu$m$^2$ were received in junctions with a layer of amorphous aluminium alloyed with niobium. These results were the logical continuation of prior experimental works on a layer of amorphous silicon alloyed with tungsten [10]. Authors call such junctions self-shunted, and in principle the limit value of $V_c = I_c R_n = \pi\Delta_{\mathrm{Nb}}/2 = 2$ mV may be achieved therein. In practice so far $V_c$ of hysteresis-free high-quality junctions does not exceed 0.3 mV.

Another important aspect in study of superconducting niobium films is anisotropy of the energy band gap. In one of the first papers [11] energy band gap anisotropy was measured on different surfaces of niobium single crystal in certain orientations. Tunnel junctions formed in different faces of such crystal with resistance ratio at different faces $R_{300}/R_4 = 178$ and higher, demonstrated minimum value of gap 2.84 meV in direction $\langle 100\rangle$, and maximum value 3.19 meV was observed in directions $\langle 311\rangle$ and $\langle 111\rangle$. In crystals with resistance ratio below 65, no anisotropy was observed, which may be related to scattering on admixtures. Gap anisotropy was observed previously by N. Zavaritskiy on stannum single crystals [12]. Maximum anisotropy of the gap is 8.4%. In a later paper by the same author [13] it was not possible to observe such anisotropy, however, the measured energy band gap was 3.12 meV. Besides, current-voltage curve demonstrated simultaneously asymmetry, knee-shaped feature and anomaly at zero shift. It is assumed that these anomalies are related to non-compensated oxygen in the boundary between niobium and oxide barrier.

It may also be noted here that for niobium the work function, i.e. the energy required for electron to exit from the metal surface into vacuum, is highly anisotropic and depends on crystal-lattice orientation of the surface [14]. For surface (100) $\Phi_{100} = 3.55$ eV, for (111) $\Phi_{111} = 3.78$ eV, for (110) $\Phi_{110} = 4.49$ eV. For polycrystalline niobium $\Phi_{\mathrm{p}} = 4.3$ eV [15]. Average barrier height at the boundary AlO$x$/Nb is determined by work functions of niobium grains with various orientations and averaged work function, therefore, the polycrystalline films demonstrate inclined gap nd knee-shaped feature as manifestation of a higher gap. To increase current density and to reduce resistance 1.2 times, it is preferable to align films with planes (100) or (111), in order to implement the lowest work function and higher transparency of the barrier.

Development of tunnel barrier in Nb/$Al_2O_3$/Nb and Al/$Al_2O_3$/Al junctions is complicated by fundamental difference of hexagonal crystal lattice of film $Al_2O_3$ and cubic structure of Nb and Al films. Attempts to make ultrathin (around 1 nm) tunnel barriers with low density of defects by method of layerwise atomic beam application [16] turn out to be hardly successful, critical current and specific voltage $V_c = 0.3$ mV turn out to be less than in theory of Ambegaokar-Baratoff (1.4 mV), which may be related to defects at the boundary.

Manufacturing of epitaxial Nb/AlN/Nb junctions on sapphire substrates [17] consisted in deposition of the first layer at 480°C, besides, addition of buffer aluminium layer 0.5 nm between AlN and upper Nb improved Nb (200) orientation and crystalline properties. Buffer layer turns niobium diffusion into barrier layer.

## 4. Aluminium films and junctions

Images of standard polycrystalline aluminium films sputtered with magnetron that are given in Fig. 4 demonstrate high roughness. These films were sputtered on oxidized silicon substrates, whose plane (001) had a layer of aluminium oxide applied, which adds roughness and prevents smooth epitaxial growth. Details for various methods are given in Table 1.

According to our measurements (Table 2), for films thinner than 20 nm the roughness is approximately half of thickness, the grain size in plan is approximately twice larger. For thicknesses 60–124 nm the roughness is 10 nm, grain size is approximately equal to thickness. Films thicker than 150 nm are smoother, roughness is around 5 nm, grain size in plan is 500 nm.

The issue of epitaxial growth of aluminium folms on sapphire is studied in detail in [18]. Films were sputtered epitaxially on a face (0001) of sapphire. Main orientation of produced films with plane (111)Al parallel to surface (0001)$Al_2O_3$ and direction [110]Al parallel to surface [1010]$Al_2O_3$. This means that tightly packed planes and directions of metal film match sublattice of oxygen ions, which results in growth of two symmetrical orientation options. In the main version tightly packed aluminium planes remain parallel to sapphire plane, but these orientations

**Table 2.** Thickness and structure of aluminium films

| Method | Thickness, nm | Roughness p/p, nm | Grain Width, nm |
|---|---|---|---|
| Hot boat | 3 | 1.8 | 8 |
| Hot boat | 6 | 3.4 | 18 |
| Hot boat | 20 | 6.7 | 40 |
| El. beam | 3 | 2.5 | 10 |
| El. beam | 60 | 7.6 | 70 |
| El. beam | 124 | 10 | 100 |
| Magnetron | 150 | 5 | 400 |

rotate relative to [110]Al axis so that $[1010]Al_2O_3$ axis is parallel either to direction [121]Al (rotation by 30°) or [541]Al (rotation by 11°). Crystal twin formation is related to two equivalent orientations of aluminium differing by rotation by 180° relative to [111]Al axis. It is not possible to produce ideally atomically smooth single-crystal film by such method.

In this paper aluminium films are grown by method of magnetron sputtering on Si(111) substrate with epitaxial seed layer. Films were deposited in two stages. First for 100 s an island layer 10–20 nm of single-crystal germs was formed on the substrate at temperature of 400°C, speed of Al particle deposition of not more than 0.2 nm/s, pressure in the chamber $1.5 \cdot 10^{-3}$ mbar and magnetron power 300 W. The process of sample cooling down to 19°C occurred under conditions of residual vacuum for 12 h. Film deposition at the second stage was carried out under the conditions of the stationary temperature of the sample. The film deposition process occurred in argon atmosphere (pressure $4 \cdot 10^{-3}$ mbar) with speed of 1.45 nm/s for time 138 s. Silicon substrate temperature was fixed at 19°C due to controlled deposition of the substrate Table from the chiller. This process is similar to the one previously practiced on the silver films. In paper [19] it was shown that transition from the stationary growth process to two-stage one made it possible to get atomically smooth single-crystal Ag/Si(111) films. The progress was achieved by formation of an island epitaxial seed layer at the boundary with the substrate at the first stage at higher growth temperature.

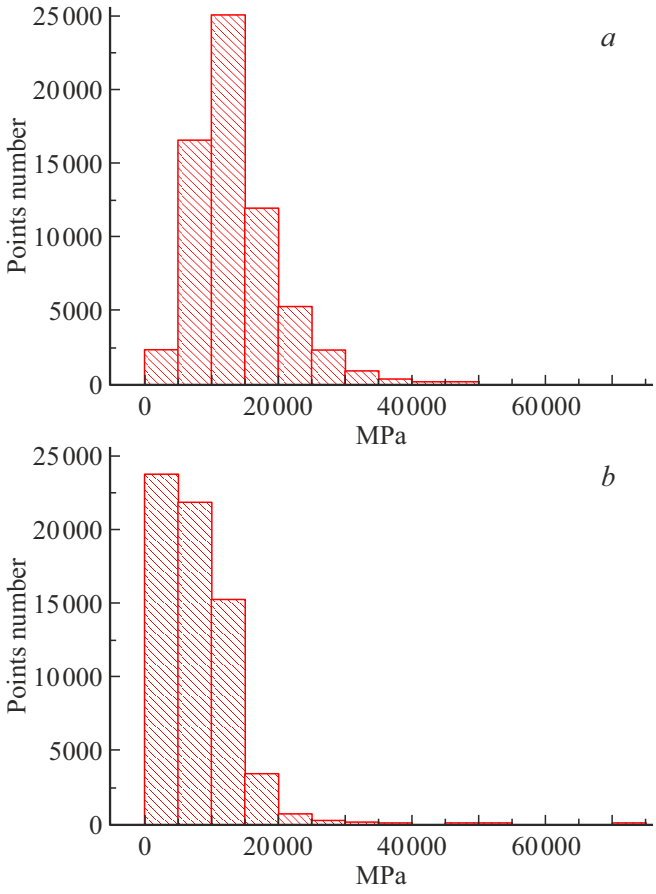


**Figure 5.** For films on the hot substrate most grains have hardness 10000–15000 MPa, and for cold ones 0–5000 MPa.

It is also useful to compare hardness of these two types of films (Fig. 5). You can see that in a hot seed layer most grains have hardness of 10000–15000 MPa, while on the cold substrate most grains have hardness of less than 5000 MPa. Higher hardness of the film sputtered on the hot germ may mean lower porosity and higher coherent length.

## 5. Discussion

Gap between theoretical knowledge of limit parameters and actual achievable values of critical current density, specific voltage, capacitance McCumber parameter, low frequency noise may be substantially reduced, if you implement the process of epitaxial growing of single-crystal films with minimum number of defects. It is important to adhere to the same cubic structure of substrate, superconductor and tunnel barrier crystals and the proximity of the lattice period.

The problem of selecting a combination of a substrate, superconductors and a dielectric is challenging, most substrates and dielectric barriers are hexagonal, and superconducting films have cubic syngony, and lattice constants differ greatly. In Table 3 there are crystalline parameters of some of used materials.

For NbN/AlN/NbN, epitaxial growth on MgO(100) substrates at temperature not higher than 100°C is quite effective. A specific feature of the process is very low speed of AlN barrier application 0.05 nm/s and low thickness of this layer. AlN barrier with thickness of less than 2 nm grows epitaxially in a cubic phase above NbN, despite their difference in volume crystalline structures. Critical current density is $250\,\mu A/\mu m^2$, $I_cR_n = 3.5$ mV [7]. Cross section STEM of such junctions demonstrates almost ideal epitaxial growth on surface (100).

Optimal manufacturing of epitaxial Nb/AlN/Nb junctions on sapphire $(Al_2O_3)$ substrates consists in deposition of the first layer at 480°C, besides, addition of buffer aluminium layer 0.5 nm between AlN and upper Nb improved Nb(200)

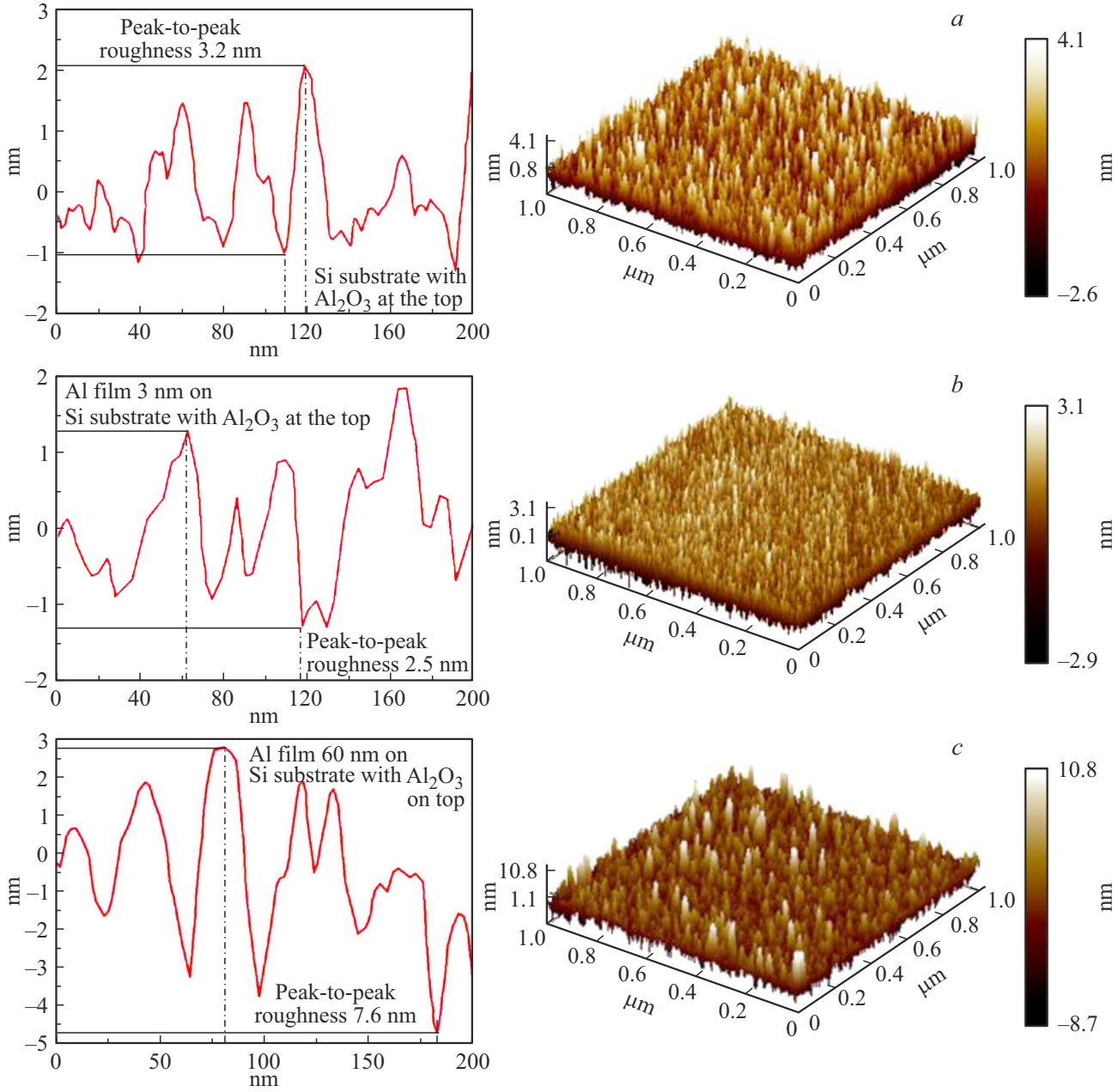


**Figure 4.** (*a*) Profile of Si substrate with sputtered insulator $Al_2O_3$. Peak-to-peak roughness 3.2 nm; (*b*) Al film with thickness 3 nm on top of that insulator. Roughness 2.5 nm (less than (*a*)); (*c*) Al film with thickness 60 nm on the same substrate. Roughness 7.6 nm.

**Table 3.** Parameters of some crystalline materials

| Material | Syngony | Lattice constant, nm | *T* melting, °C | Density, g/cm$^3$ |
|---|---|---|---|---|
| Nb | cubic | 0.33 | 2468 | 8.6 |
| Al | cubic | 0.4 | 660 | 2.7 |
| NbN | cubic (hg) | 0.44 (0.3; 0.57) | 2300 | 8.4 |
| $NbTiN_2$ | cubic (th) | 0.44 (0.44; 0.87) | | |
| $Al_2O_3$ | hexagonal (trig) | 0.47; 0.47 1.3 | 2050 | 4 |
| $SiO_2$ | trigonal | 0.31 | 1713 | 2.6 |
| AlN | hexagonal (cub) | 0.31; 0.5 | 2200 | 3.2 |
| MgO | cubic | 0.42 | 2825 | 3.6 |
| Si | cubic | 0.54 | 1414 | 2.3 |

orientation and crystalline properties. Buffer layer turns niobium diffusion into barrier layer.

Optimal process of forming Al/AlO$x$/Al and Al/AlN/Al structures consists in epitaxial growth of aluminium film in two stages by method of magnetron sputtering on Si(111) substrate with epitaxial seed layer. First for 100 s an island layer 10−20 nm of single-crystal germs was formed on the substrate at temperature of 400°C, speed of Al particle deposition of not more than 0.2 nm/s. The process of sample cooling down to 19°C occurred under conditions of residual vacuum for 12 h. Film deposition at the second stage was carried out under the conditions of the stationary temperature of the sample. The process of deposition of the main film 150 nm occurs in the argon atmosphere with speed of 1.45 nm/s for time 138 s at substrate temperature 19°C. Formation of a thin barrier layer happens with low speed to form a cubic phase (and not hexagonal one at increased thickness).

In all listed cases the principal approach consists in formation of epitaxial structure of cubic syngony for all layers: substrate, first superconductor, tunnel barrier, second superconductor. In this case it is possible to achieve both high-high values of current density and minimum specific capacitance of the tunnel junction.

## Funding

Samples were developed and studied in the Institute of Radio Technologies and Electronics of the Russian Academy of Science with grant by the Russian Scientific Fund No. 21-42-04421, https://rscf.ru/project/21-42-04421/. Experimental samples were made within a state assignment by the Institute of Radio Technologies and Eletronics named after V.A. Kotelnikov of the Russian Academy of Science. The work for analysis of multilayer structures was performed under the State Assignment to the Valiev Institute of Physics and Technology of the Russian Academy of Sciences from the Ministry of Education and Science of the Russian Federation, project No. FFNN-2022-0019. Samples were made with equipment of the unique scientific plant № 352529 „Cryointegral“, supported by grant of the Ministry of Science and Higher Education of the Russian Federation under agreement 075-15-2021-667. AFM measurements were made in the Institute of Biomedical Chemistry named after V.N. Orekhovich using unique scientific plant „Avogadro“ CUC „Human Proteome“, which is supported by the Ministry of Science and Higher Education of the Russian Federation (Agreement No. 075-15-2021-993).

## Conflict of interest

The authors declare that they have no conflict of interest.

## References

[1] T. Greibe, M. Stenberg, C. Wilson, T. Bauch, V. Shumeiko, P. Delsing. Phys. Rev. Lett. **106**, 097001 (2011).
[2] M. Tarasov, A. Chekushkin, M. Fominsky, D. Zakharov, A. Lomov, O. Devitsky, A. Gunbina, E. Sokhina, V. Edelman. FTT **64**, *10*, 1369 (2022). (in Russian). DOI: 10.21883/0000
[3] L. Solymar. Superconductive tunneling and applications. C.&H Ltd, London. 406 p., SBN 412 10210 2 (1972).
[4] Z. Wang, A. Kawakami, Y. Uzava, B. Komiyama. J. Appl. Phys. **79**, *10*, 78377842 (1996).
[5] S. Lloyd, D. Tricker, Z. Barber, M. Blamire. Phil. Mag. A **81**, *10*, 2317 (2001).
[6] T. Polakovic, S. Lendinez, J. Pearson, A. Hoffmann, V. Yefremenko, C. Chang, W. Armstrong. APL Mater. **6**, 076107 (2018). DOI: 10.1063/1.5031904
[7] Z. Wang, H. Terai, W. Qiu, K. Makise, Y. Uzawa, K. Kimoto, Y. Nakamura. Appl. Phys. Lett. **102**, *14*, 142604 (2013).
[8] S. Tolpygo, D. Yohannes, R. Hunt, J. Vivalda, D. Donnelly, D. Amparo, A. Kirichenko. IEEE TAS **17**, *2*, 946 (2007).
[9] S. Tolpygo, V. Bolkhovsky, D. Oates, R. Rastogi, S. Zarr, A. Day, T. Weir, A. Wynn, L. Johnson. IEEE TAS **28**, *4*, 1100212 (2018).
[10] A. Gudkov, M. Kupriyanov, K. Likharev. Sov. Phys. JETP **68**, *1*, 1478 (1988).
[11] M. MacVicar, R. Rose. J. Appl. Phys. **39**, *3*, 1721 (1968).
[12] N.V. Zavaritskii. Soviet Phys. JETP **18**, 1260 (1965). Soviet Phys. JETP **21**, 557 (1964).
[13] J. Bostock, K. Agyeman, M. Frommer, M. MacVicar. J. Appl. Phys. **44**, *12*, 5567 (1973).
[14] J. Wang, S.-Q. Wang. Surf. Sci. **630**, 216 (2014).
[15] H. B. Michaelson. J. Appl. Phys. **48**, *11*, 4729 (1977).
[16] R. Lu, A. Elliot, L. Wille, Bo Mao, S. Han, J. Wu, J. Talvacchio, H. Schulze, R. Lewis, D. Ewing, H. Xue, S. Zhao. IEEE TAS **23**, *3*, 1100705 (2013).
[17] Y. Tanaka, D. Sato, F. Shimada, Y. Nakada, A. Saito. Fabrication and evaluation of epitaxial Nb/AlN/Nb junctions with Al buffer layers. EUCAS2021, Sept. 5−9, Moscow, (2021).
[18] D. Medlin, K. McCarty, R. Hwang, S. Guthrie, M. Baskes. Thin Solid Films **299**, 110 (1997).
[19] I.A. Rodionov, A.S. Baburin, A.R. Gabidullin, S.S. Maklakov, S. Peters, I.A. Ryzhikov, A.A. Andriyash. Sci. Rep. **9**, 12232 (2019).